CONF-8906270--5

DISCLAIMER

This report was prepared as an account of work sponsored by an agency of the United States Government. Neither the United States Government nor any agency thereof, nor any of their employees, makes any warranty, express or implied, or assumes any legal liability or responsibility for the accuracy, completeness, or usefulness of any information, apparatus, product, or process disclosed, or represents that its use would not infringe privately owned rights. Reference herein to any specific commercial product, process, or service by trade name, trademark, manufacturer, or otherwise does not necessarily constitute or imply its endorsement, recommendation, or favoring by the United States Government or any agency thereof. The views and opinions of authors expressed herein do not necessarily state or reflect those of the United States Government or any agency thereof.

THE THEORY OF ELECTRON-ION COLLISIONS: THE ROLE OF DOUBLY EXCITED STATES

CONF-8906270--5

DE90 011078

D. C. Griffin
Department of Physics, Rollins College
Winter Park, Florida 32789

M. S. Pindzola
Department of Physics, Auburn University
Auburn, Alabama 36849

C. Bottcher
Physics Division, Oak Ridge National Laboratory
Oak Ridge, Tennessee 37831

ABSTRACT

The important contributions of doubly excited autoionizing states to electron-impact excitation, ionization, and recombination are reviewed. Various theoretical methods of treating these states are considered, and theoretical cross sections are presented and compared to experimental measurements where available.

1. INTRODUCTION

Doubly excited states play a major role in electron-ion collisions. If such states are above the first ionization limit of an N-electron ion, they interact with the adjacent continuum and can decay by the de-excitation of one electron and the simultaneous ejection of a second electron, resulting in the production of an (N-1)-electron ion. However, in addition to this process of autoionization, they can also decay to a bound state of the

MASTER

DISTRIBUTION OF THIS DOCUMENT IS UNLIMITED

N-electron ion, with the emission of a photon.

They may be populated from the N-electron ion by the excitation of an inner-shell electron or the excitation of two valence-shell electrons, or from the (N-1)-electron ion by the excitation of one bound electron and the simultaneous capture of a free electron. We refer to this last process as resonant recombination; it is just the reverse of autoionization. These processes, which are part of the indirect mechanisms in electron impact-excitation, ionization, and recombination, are depicted schematically in Fig. 1.

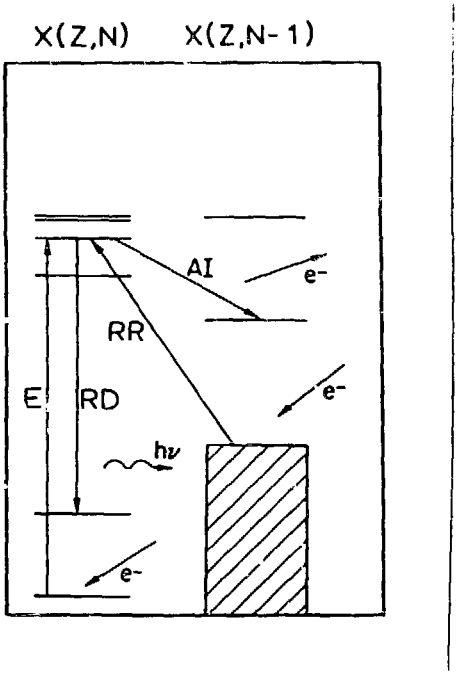

Fig. 1. Schematic drawing showing the population and decay of a doubly excited state of an ion X(Z,N) with atomic number Z and N electrons. It can be populated by excitation (E) of the N-electron ion or resonant recombination (RR) from the (N-1)-electron ion, and can decay by autoionization (AI) or radiative decay (RD).

Since these doubly excited states are coupled to the adjacent continuum, and through the continuum to each other, one should properly treat such processes by

constructing a wavefunction which is some linear combination of states consisting of N bound orbitals with states consisting of N-1 bound orbitals and one continuum orbital. However, in many cases, one can employ an independent-processes model and treat the interaction with the continuum using perturbation theory.

2. ELECTRON-IMPACT EXCITATION

The contribution of doubly excited autoionizing states to electron-impact excitation can be included in a very natural way through the use of the close-coupling approximation. One begins by obtaining a set of bound-state eigenfunctions and eigenvalues which describe the target states of an (N-1)-electron ion

$$H_{N-1}\chi_i(x_1 \cdots x_{N-1}) = E_i\chi_i(x_1 \cdots x_{N-1}), \qquad (1)$$

where x_i denotes the space and spin coordinates. The radial wavefunctions for the bound-state orbitals can be obtained from the Hartree-Fock approximation, and the energy eigenvalues, E_i, and the eigenvectors, χ_i, are determined by diagonalizing the Hamiltonian matrix for the (N-1)-electron system including the effects of configuration interaction.

The wavefunction for the N-electron collision problem is then constructed from vector-coupled antisymmetized products of the (N-1)-electron wavefunctions with a spin-orbital of the form

$$\theta(\ell_i m_{\ell_i} m_{s_i} | x) = Y_{\ell_i m_{\ell_i}}(r)\delta(m_{s_i}, \sigma_i)\,\frac{1}{r}\,F_i(r), \qquad (2)$$

where $Y_{\ell m}$ is a spherical harmonic, σ is a spin coordinate, and $F_i(r)$ describes the radial part of the wavefunction for

the N'th electron when the ion is in the state i.

For atomic systems with low Z, we can ignore the spin-orbit interaction, as well as other relativistic effects, and the conserved quantum numbers are $(LS\Pi)$, where L is the total orbital angular momentum, S is the total spin angular momentum, and Π is the parity of the N-electron system. The state i of the (N-1)-electron ion in LS-coupling is specified by the quantum numbers $\alpha_i L_i S_i M_{L_i} M_{S_i}$, where α_i represents all other quantum numbers needed to completely specify the state. One then forms wavefunctions for each channel, i, from the vector-coupled antisymmetrized product functions

$$\Theta_i = \sum_{\substack{M_{L_i} m_{\ell_i} \\ M_{S_i} m_{s_i}}} C^{L_i \ell_i L}_{M_{L_i} m_{\ell_i} M_L} \, C^{S_i 1/2 S}_{M_{S_i} m_{s_i} M_S} \, Ax(\alpha_i L_i S_i M_{L_i} M_{S_i} | x_1 \cdots x_{N-1}) \, \theta(\ell_i m_{\ell_i} m_{s_i} | x_N) \ , \tag{3}$$

where A is the operator that antisymmetrizes the total wavefunction.

In the close-coupling (CC) approximation, the total wavefunction is taken to be a finite expansion over the wavefunctions for each channel

$$\Psi(x_1 \cdots x_N) = \sum_i \Theta_i \ . \tag{4}$$

In the most widely used formulation of the CC approximation, one also explicity includes a set of N-electron bound-state functions in the above expansion. These so-called correlation functions are necessary to remove a constraint on the total wavefunction if one insists on orthogonality between the bound-state radial functions and the radial function $F_i(r)$. However, for simplicity, we will consider the form of the CC equations

when one does not impose this condition.

Application of the variational principle leads to a set of coupled differential equations, which in atomic units are of the form

$$\left[-\frac{1}{2}\frac{d^2}{dr^2} + \frac{\ell_i(\ell_i+1)}{2r^2} - \frac{Z}{r} + V_{ii} - \frac{k_i^2}{2} \right] F_{ii'}(r) + \sum_{j \neq i} V_{ij} F_{ji'}(r) = 0, \qquad (5)$$

where we now employ a double index on the radial function $F_{ii'}(r)$ to denote the incident channel i', and the channel index i now signifies the collection of quantum numbers $\alpha_i L_i S_i k_i \ell_i L S \pi$. The potential function V_{ij} contains both direct and exchange electrostatic terms, as well as exchange overlap terms which arise because of the non-zero overlap between the bound orbitals and the radial functions $F_{ii'}(r)$ with the same orbital angular momentum.

For open channels for which $k_i^2 > 0$, the asymptotic form of the radial wavefunction may be written in the form

$$F_{ii'}(r)_{r\to\infty} \sim \frac{1}{\sqrt{k_i}} \left[\delta_{ii'} \sin k_i x + R_{ii'} \cos k_i x \right] , \qquad (6)$$

where $k_i x = k_i r - \ell_i \pi/2 + (z/k_i)\ln(2k_i r) + \arg\Gamma[\ell_i+1-i(z/k_i)]$, with $z=Z-N+1$, is the asymptotic phase of the regular Coulomb function, and $R_{ii'}$ is an element of the reactance matrix R. For closed channels with $k_i^2 < 0$, we require that $F_{ii'}(r) \longrightarrow 0$ as $r \longrightarrow \infty$.

The cross section for the excitation $\alpha_i L_i S_i \longrightarrow \alpha_f L_f S_f$ in atomic units is given by

$$\sigma_{if} = \frac{\pi}{k_i^2\, 2(2L_i+1)(2S_i+1)} \sum_{LS\ell_i\ell_f} (2L+1)(2S+1) \left| T_{fi} \right|^2 , \quad (7)$$

where T_{fi} is an element of the transition matrix T, which is related to the reactance matrix R by the equation

$$T = \frac{-2iR}{(1 - iR)} . \quad (8)$$

For initial electron energies where both open and closed channels are included in the wavefunction expansion, we obtain Feshbach or closed-channel resonances. For example, consider the idealized system shown in Fig. 2 with the (N-1)-electron ion initially in the ground state i. The incident electron energy ε_i is such that channels associated with level f are open, but those associated with level c are closed. The incident electron can be captured (resonant recombination) into the doubly excited autoionizing state j consisting of a Rydberg electron attached to the (N-1)-electron core in level c. This state can: (1) autoionize to the initial state i, and we have a resonance in the elastic cross section; (2) autoionize to the excited state f, with the emission of an electron of energy ε_f, and we have a resonance in the excitation cross section; or (3) it can radiatively decay to a bound state b and contribute to the recombination (dielectronic) cross section. In order to include this last process, which of course reduces the size of the resonance contributions to the scattering cross sections, the interaction with the radiation field would have to be included in the close-coupling formalism.

Resonances can make significant contributions to the excitation cross section. For example, the cross section resulting from a 6-state (4s, 3d, 4p, 5s, 4d, 5p) close-coupling calculation[1)] for the transition 4s→3d in Ca^+ is

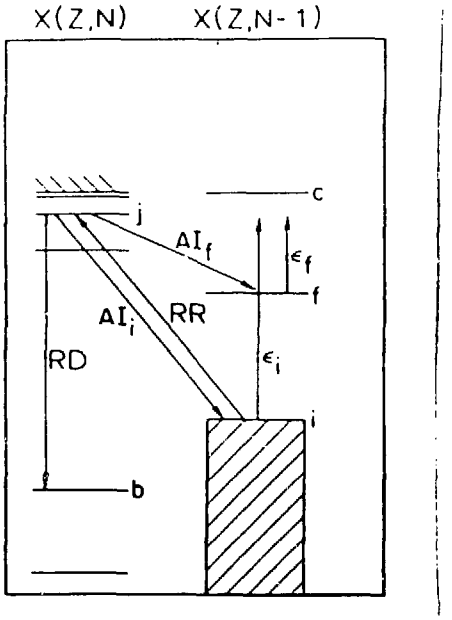

Fig. 2. Schematic drawing of an idealized resonant system. The initial electron with energy $\varepsilon_i=k_i^2/2$ can be captured (RR) into a doubly excited state j. This state can then autoionize to the initial state i [AI_i], or the excited state f [AI_f] (ejecting an electron of energy $\varepsilon_f=k_f^2/2$); or radiatively decay (RD) to a bound state b.

shown in Fig. 3. Resonances, especially from the doubly excited states of the type 4pnℓ, dominant the cross section for incident electron energies between the 3d and 4p thresholds.

As the net ionic charge increases, the spin-orbit interaction becomes large, and the LS representation is no longer valid. The close-coupling approximation must then be formulated in terms of channels associated with individual intermediate-coupled levels, rather than LS terms. For a complex ion there may be a large number of levels which should be included in a single calculation, and solving the coupled equations becomes a formidable task. However, for many cases in highly ionized species, the coupling between open channels is weak,[2] and one is justified in employing the much simpler distorted-wave (DW)

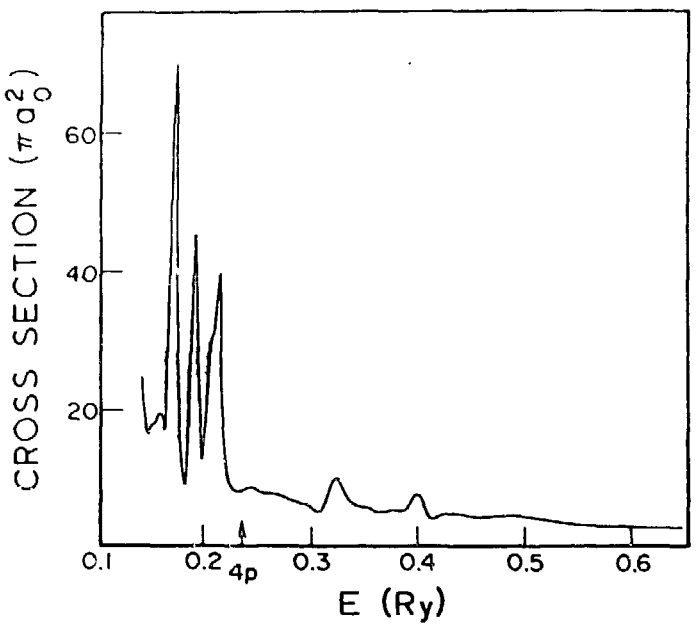

Fig. 3. The excitation cross section (in units of πa_0^2) for the 4s→3d transition in Ca^+ from a 6-state close coupling calculation.[1] The 3d threshold is at .125 rydbergs and the 4p threshold, at .231 rydbergs, is indicated by the small arrow along the energy axis.

approximation to determine the direct-excitation cross section. We drop all potential terms V_{ij} with $i \neq j$ in Eq. (5) and solve the DW differential equation

$$\left[-\frac{1}{2}\frac{d^2}{dr^2} + \frac{\ell_i(\ell_i+1)}{2r^2} - \frac{Z}{r} + V_{ii} - \frac{k_i^2}{2} \right] f_i(r) = 0 , \qquad (9)$$

where the asymptotic form of the radial wavefunction, $f_i(r)$, is

$$f_i(r) \underset{r\to\infty}{\sim} \sin(k_i x + \delta_i) , \qquad (10)$$

and where δ_i is the distorted-wave phase shift. The cross section for the transition $\alpha_i J_i \rightarrow \alpha_f J_f$ between two levels of total angular momentum J_i and J_f is given by

$$\sigma_{if} = \frac{4\pi}{k_i^2(2J_i+1)} \sum_{\substack{J\ell_i\ell_f \\ j_i j_f}} (2J+1) \, | \rho_{fi} |^2 , \tag{11}$$

where J is the total angular momentum of the N-electron system, $j_i=\ell_i\pm1/2$, $j_f=\ell_f\pm1/2$, and ρ_{fi} is an element of the ρ matrix, with off-diagonal elements given by

$$\rho_{fi} = \frac{-2}{\sqrt{k_i k_f}} \int_0^\infty f_f(r) V_{fi} f_i(r) dr , \tag{12}$$

and diagonal elements equal to zero.

Although, for highly ionized species, continuum coupling may have a small effect on the direct-excitation cross section, the contribution of resonances to the total-excitation cross section is still quite important. Thus it would be advantageous to include the effects of resonances within the distorted-wave formalism. If the coupling of the resonances to the adjacent continuum is relatively weak, we can impose the independent-processes approximation, and use perturbation theory to show that the total cross section from a level i to a level f is given by

$$\sigma_t(i \rightarrow f) = \sigma_d(i \rightarrow f) + \sum_j \sigma_r(i \rightarrow j) B^a(j \rightarrow f) , \tag{13}$$

where $\sigma_d(i \rightarrow f)$ is the direct-excitation cross section from level i to level f, calculated from Eq. (11); $\sigma_r(i \rightarrow j)$ is the resonant-recombination cross section from level i of the (N-1)-electron ion to the doubly excited level j of the N-electron ion; and $B^a(j \rightarrow f)$ is the branching ratio for autoionization from level j to level f. $B^a(j \rightarrow f)$ is given by the equation

$$B^a(j \rightarrow f) = \frac{A_a(j \rightarrow f)}{\sum_k A_a(j \rightarrow k) + \sum_n A_r(j \rightarrow n)} , \qquad (14)$$

where $A_a(j \rightarrow k)$ is the autoionizing rate from level j to a lower level k of the (N-1)-electron ion, and $A_r(j \rightarrow n)$ is the radiative rate from level j to a bound level n of the N-electron ion.

By the principle of detailed balance, the resonant-recombination cross section from level i to level j, averaged over a narrow energy bin, can be written in terms of the rate for the reverse process of autoionization from level j to level i as

$$\sigma_r(i \rightarrow j) = \frac{2\pi^2}{\Delta\varepsilon k_i^2} \frac{2J_j+1}{2(2J_i+1)} A_a(j \rightarrow i) , \qquad (15)$$

where J_i and J_j are the total angular momenta of levels i and j, respectively, and $\Delta\varepsilon$ is an energy bin width larger than the largest resonance width. The autoionizing rates are calculated using distorted-wave continuum functions and the autoionizing and radiative rates necessary for the determination of resonant contributions from high Rydberg states are found by extrapolating calculated rates.

This formalism was first used by Cowan[3] to determine the resonant contributions to the $(2s^2)^1S \rightarrow (2s2p)^3P$ excitation in O^{4+}. He obtained good agreement with close-coupling calculations. Since then, it has been used to determine the resonant contribution to excitation for a number of highly ionized systems. For example, we employed this method[4] to estimate the resonant contribution from doubly excited states of the form $2p^5 3pn\ell$, $2p^5 3dn\ell$, and $2p^5 4\ell 4\ell'$ to the relatively weak transition $2p^6 \rightarrow 2p^5 3s$ in Ti^{12+}. The results are shown in Fig. 4, where the indirect cross sections, averaged over a narrow energy bin $\Delta\varepsilon$, were

convoluted with a gaussian distribution function typical of experimental electron distributions. Obviously, the resonant contributions dominate the cross section.

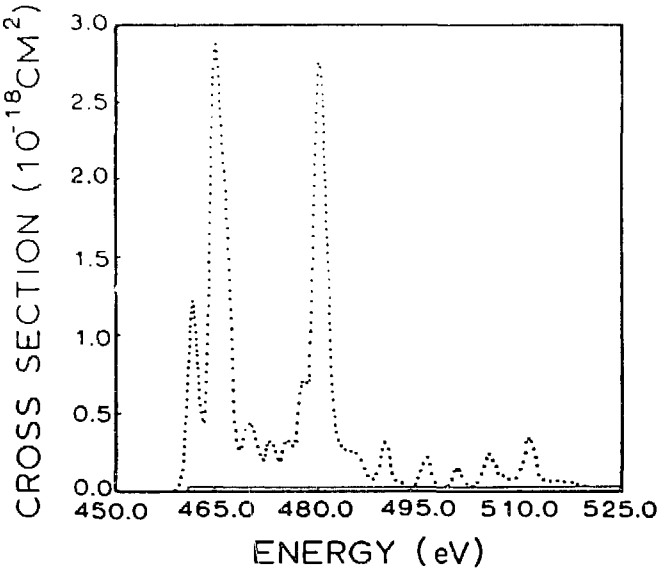

Fig. 4. Electron-impact $2p^6 \longrightarrow 2p^5 3s$ excitation cross section of Ti^{12+}. The solid curve, hardly visible on the scale of the graph, is the direct-excitation cross section, while the dotted curve is the sum of the direct and indirect cross sections.

3. ELECTRON-IMPACT IONIZATION

We now consider the electron-impact ionization of an N-electron ion X(Z,N). The direct-ionization process is

$$e^- + X(Z,N) \longrightarrow X(Z,N-1) + e^- + e^- \ . \qquad (16)$$

However, in addition, we can have the indirect processes of inner-shell excitation followed by autoionization

$$e^- + X(Z,N) \longrightarrow X(Z,N)^{**} + e^-$$
$$\hookrightarrow X(Z,N-1) + e^- \ ; \qquad (17)$$

resonant recombination to a doubly excited state of the (N+1)-electron ion followed by the sequential autoionization of two electrons

$$e^- + X(Z,N) \longrightarrow X(Z,N+1)^{**} \longrightarrow X(Z,N)^{**} + e^- \longrightarrow X(Z,N-1) + e^- \; ; \qquad (18)$$

and resonant recombination followed by the simultaneous autoionization of two electrons

$$e^- + X(Z,N) \longrightarrow X(Z,N+1)^{**} \longrightarrow X(Z,N-1) + e^- + e^- \; . \qquad (19)$$

The double asterisk in the above equations denotes a doubly excited autoionizing state.

For now we consider only the first two processes of direct ionization and excitation autoionization. If one employs an independent-processes approximation, the total ionization cross section from an initial configuration i is given by

$$\sigma_{tot}(i) = \sum_f \sigma_{ion}(i \rightarrow f) + \sum_j \sigma_{exc}(i \rightarrow j) B_j^a \; , \qquad (20)$$

where $\sigma_{ion}(i \rightarrow f)$ is the distorted-wave direct-ionization cross section from the initial configuration i to the final configuration f of the (N-1)-electron ion, and $\sigma_{exc}(i \rightarrow j)$ is the distorted-wave inner-shell excitation cross section from configuration i to a particular doubly excited level j. B_j^a is the branching ratio for autoionization to all lower levels of the (N-1)-electron ion, which is given by

$$B_j^a = \frac{\sum_k A_a(j \rightarrow k)}{\sum_k A_a(j \rightarrow k) + \sum_n A_r(j \rightarrow n)} . \tag{21}$$

There is a particular difficulty with the calculation of the direct-ionization cross section $\sigma_{ion}(i \rightarrow f)$ which is important to mention. It is associated with the fact that the final state involves two free electrons in the field of an ion, which is a problem in many-body theory that has not yet been solved in a manner suitable for practical calculations. In the distorted-wave approximation, it is assumed that each of two electrons experiences a spherical potential at infinity; thus, the phase between the two electrons is lost, and the relative phase between the direct and exchange terms within the cross-section formula is unknown. We employ the minimum-phase approximation of Peterkop[5]) which amounts to squaring the difference between the absolute values of the direct and exchange amplitudes; this leads to maximum destructive interference and seems to give the best agreement with experiment.

We have performed numerous calculations of total-ionization cross sections for highly ionized species using this approximation. However, in principle, one should include the possible quantum mechanical interference between direct ionization and excitation autoionization. Jakubowicz and Moores[6]) have developed a method of doing this by using either Coulomb or distorted waves to represent the scattered electron, but close-coupling wavefunctions to describe the N-electron target states, before and after the collision. In this way, they include the interaction between the doubly excited autoionizing states and the adjacent continuum explicitly. However, the good agreement between calculations performed using this method[7]) with those performed using the independent-

processes approximation[8] seems to indicate that interference between direct ionization and excitation autoionization has a small effect on the total-ionization cross section.

Excitation autoionization can dominate over direct ionization, even for highly ionized species. For example, consider ionization of Na-like ions from the $2p^6 3s$ ground state. In addition to direct ionization out of the 3s, 2p, and 2s subshells, we can have indirect contributions from inner-shell excitation to doubly excited configurations of the type $2s^2 2p^5 3sn\ell$ and $2s2p^6 3sn\ell$. Calculations for the ions Ti^{11+}, Cr^{13+}, Fe^{15+}, and Ni^{17+} using the independent-processes approximation[9] indicate that the excitation-autoionization contributions enhance the total cross section near threshold by nearly a factor of five, in agreement with cross-beam measurements for the first three of these ions.[10,11]

In Fig. 5, we show the calculated[9] and measured[11]

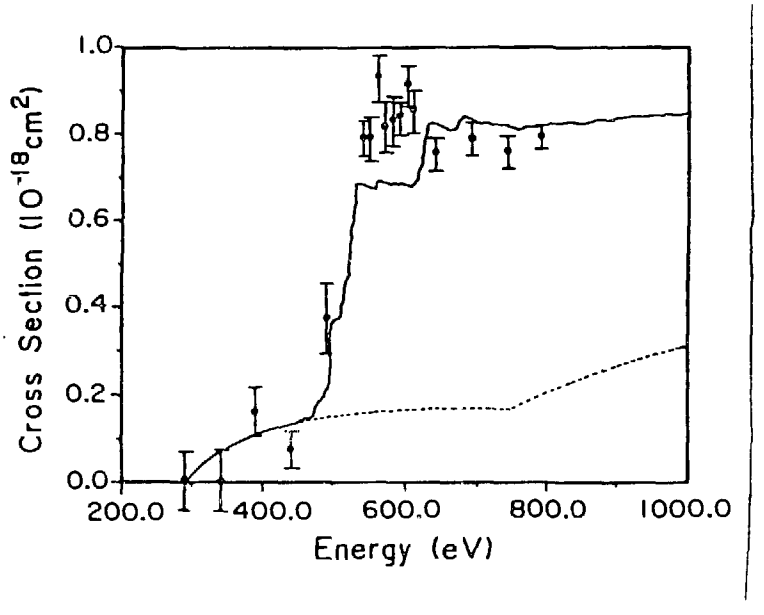

Fig. 5. Calculated ionization cross section for Ti^{11+}. Solid curve, total-ionization cross section; dashed curve, direct-ionization contributions only. Experimental points are from Ref. 11.

cross sections for Ti^{11+}. The overall agreement between experiment and theory is good; however, the data points are clearly above the calculated cross section in the energy range from about 550 eV to 610 eV. This may indicate the formation of recombination resonances of the type $2s^2 2p^5 3sn\ell n'\ell'$ and $2s2p^6 3sn\ell n'\ell'$ in Ti^{10+}, which can autoionize sequentially with the emission of two electrons to Ti^{12+} (see Eq. 18).

In the independent-processes approximation, the cross section for this process of resonant recombination double autoionization (RRDA) is given by

$$\sigma_{rrda} = \sum_j \sigma_r(i \rightarrow j) B_j^{da}, \tag{22}$$

where $\sigma_r(i \rightarrow j)$ is the resonant-recombination cross section from level i of the N-electron ion to a particular doubly excited level j of the (N+1)-electron ion (Eq. 15). B_j^{da} is the branching ratio for double autoionization, which is given by

$$B_j^{da} = \sum_d \left[\frac{A_a(j \rightarrow d)}{\sum_k A_a(j \rightarrow k) + \sum_n A_r(j \rightarrow n)} \times \frac{\sum_f A_a(d \rightarrow f)}{\sum_f A_a(d \rightarrow f) + \sum_m A_r(d \rightarrow m)} \right], \tag{23}$$

where the first term inside the square brackets is the branching ratio for autoionization to a particular doubly excited autoionizing level d of the N-electron ion; the second term is the branching ratio for autoionization from the level d to any lower level of the (N-1)-electron ion; and finally, the sum over k in the first term includes autoionization to all lower levels of the N-electron ion,

both autoionizing and bound.

Because of the extremely large number of levels involved in the determination of the double autoionization branching ratios, such a calculation for a case like that of Ti^{11+} becomes very difficult to perform, even at this level of approximation. LaGattuta and Hahn[12] employed average rates between configurations, rather than between individual levels, to obtain an estimate for RRDA in Na-like Fe^{15+}, but comparison with experiment[10] indicates that this method far over estimates the contribution of the resonances. Chen and Reed[13] have just completed a very large calculation of the RRDA process for Fe^{15+} between the individual levels, and they find that the size of the resonance contribution to the ionization cross section agrees well with the experimental measurement.[10]

Now consider the resonant-recombination process followed by the simultaneous emission of two electrons (Eq. 19). We shall refer to this as resonant recombination auto-double ionization (RRAD). The cross section for RRAD is given by

$$\sigma_{rrad} = \sum_j \sigma_r(i \rightarrow j) B_j^{ad}, \tag{24}$$

where B_j^{ad} is the branching ratio for auto-double ionization

$$B_j^{ad} = \frac{\sum_f A_{ad}(j \rightarrow f)}{\sum_f A_{ad}(j \rightarrow f) + \sum_k A_a(j \rightarrow k) + \sum_n A_r(j \rightarrow n)}, \tag{25}$$

and where $A_{ad}(j \rightarrow f)$ is the auto-double ionization rate from the doubly excited level j the (N+1)-electron ion to level f of the (N-1)-electron ion.

Auto-double ionization is strictly an electron-electron correlation effect, since it involves de-excitation of one electron and the simultaneous ejection of

two electrons. We have used many-body perturbation theory to estimate the contribution of RRAD to the ionization cross section of Li-like ions.[14] In particular we considered the the RRAD process

$$e^- + 1s^2 2s \longrightarrow (1s2s^2 2p)^3P \longrightarrow 1s^2 + e^- + e^- . \qquad (26)$$

The $(1s2s^2 2p)^3P$ term of the corresponding Be-like ion was chosen because there exist no open channels for sequential double autoionization, and because of its relative simplicity. The term $(1s2s^2 2p)^1P$ was not included because it has a very small resonant-recombination cross section.

The auto-double ionization rate was calculated in lowest-order perturbation theory by summing up over a large number of continuum and bound intermediate states. As in the case of direct ionization, the final state involves two continuum electrons, and the phase between the direct and exchange terms is unknown. In order to obtain a range of possible rates, we used a set of different phase choices. The minimum rate was obtained by using the minimum-phase approximation, similar to that used in direct-ionization calculations, in which one squares the difference between the absolute values of the direct and exchange amplitudes. The maximum rate was obtained by employing the maximum-phase approximation, in which one squares the sum of the absolutes values of the direct and exchange amplitudes.

Although our calculations indicated that the contribution from this RRDA process should be a maximum of only 0.64% of the direct ionization cross section in C^{3+}, the resonant contributions from the terms $(1s2s^2 2p)^3P$ and $(1s2s2p^2)^3D$ to the ionization cross section of this ion were recently measured by Müller et al. at Giessen.[15] Their measured cross section for the $(1s2s^2 2p)^3P$ resonance was 1.1×10^{-20} cm^2, while our calculated cross section was 0.96×10^{-20} cm^2 using the minimum-phase approximation and

1.7×10^{-20} cm^2 using the maximum-phase approximation.

Müller et al.[16] have just completed an experiment on the ionization of Li^+, in which they observed the indirect processes of double excitation followed by autoicniation

$$e^- + Li^+(1s^2) \longrightarrow Li^+(2\ell 2\ell') + e^- \quad \hookrightarrow Li^{2+}(1s) + e^- , \qquad (27)$$

and double excitation with resonant recombination followed by auto-double ionization

$$e^- + Li^+(1s^2) \longrightarrow Li(2\ell^2 2\ell') \longrightarrow Li^{2+}(1s) + e^- + e^- . \qquad (28)$$

Shown in Fig. 6 is the total-ionization cross section, minus the background direct-ionization cross section, from

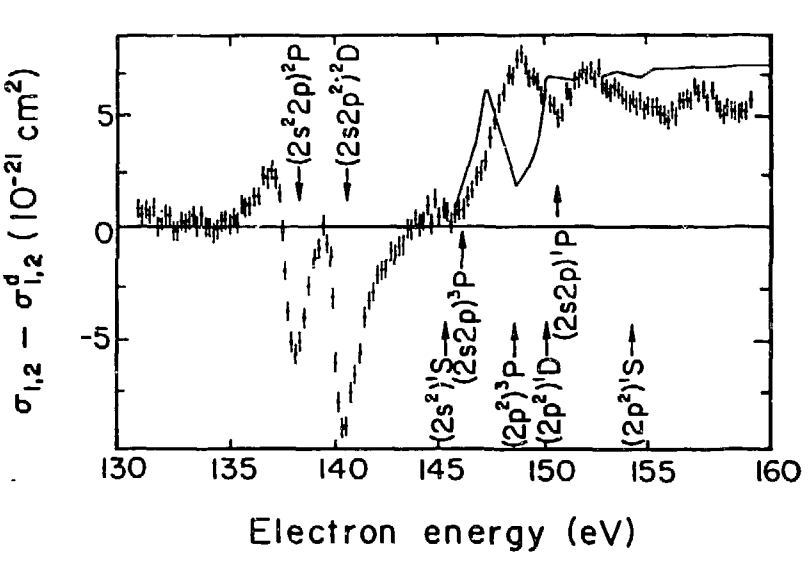

Fig. 6. The data points from Müller et al.[16] show the total-ionization cross section minus the direct-ionization cross section for Li^+ in the energy range where indirect processes contribute. The solid curve is the cross section for the $1s^2 \longrightarrow 2\ell 2\ell'$ double excitation from an 11-state close-coupling calculation. The positions of the $(2s^22p)^2P$ and $(2s2p^2)^2D$ terms of Li are from Ref. 16, while the positions of the doubly excited states of Li^+ were obtained from Hartree-Fock calculations with configuration interaction.

this experiment in the energy range where these indirect processes contribute. The shape of the curve where the recombination resonances $(2s^2 2p)^2P$ and $(2s2p^2)^2D$ can be populated indicates strong interference with the direct-ionization background. A theoretical description of the interference between these processes involving a double-electron continuum has not yet been worked out; however, the shape of the curve closely resembles the familiar Fano profile, even though Fano theory[17] applies only to a doubly excited state interfering with a single-electron continuum.

In order to investigate the process of double excitation followed by autoionization (Eq. 27), we performed an 11-state close-coupling calculation [$(1s^2)^1S$, $(1s2s)^3S$, $(1s2s)^1S$, $(1s2p)^3P$, $(1s2p)^1P$, $(2s^2)^1S$, $(2s2p)^3P$, $(2s2p)^1P$, $(2p^2)^3P$, $(2p^2)^1D$, and $(2p^2)^1S$] of the cross section for the $1s^2 \longrightarrow 2\ell 2\ell'$ double excitation. The 1s orbital, was obtained from a Hartree-Fock calculation of the $1s^2$ configuration, while the 2s and 2p orbitals were from Hartree-Fock calculations for the 1s2s and 1s2p configurations, respectively. Although, these particular 2s and 2p orbitals were used in performing the close-coupling calculations, they give poor energies for the doubly excited terms; therefore the positions of these terms were determined from a configuration-interaction calculation using 2s and 2p orbitals obtained from Hartree-Fock calculations for the $2s^2$ and $2p^2$ configurations. The close-coupling calculations were carried out using the program IMPACT.[18] The branching ratios for autoionization to the $1sk\ell$ continuum for these doubly excited states are equal to one.

The results of this calculation are shown by the solid curve in Fig. 6. The magnitude of the calculated cross section is in reasonable agreement with the experiment above the last doubly excited state. However, the shape of

the calculated cross section, near the excitation threshold, is quite different from the measurement. In addition the calculation includes contributions from recombination resonances of the type $2\ell 2\ell' n\ell''$, which may, or may not, contribute to the ionization cross section, depending on the branching ratios for double autoionization (Eq. 23). Thus, a great deal more work will be required to properly treat this process. Obviously, these new ionization experiments are severly testing the current state of electron-ion collision theory.

4. ELECTRON-IMPACT RECOMBINATION

Finally we consider the recombination of free electrons with an (N-1)-electron ion. The first process is three-body recombination

$$e^- + e^- + X(Z,N-1) \longrightarrow X(Z,N) + e^- \ . \tag{29}$$

It is just the reverse of electron-impact ionization, and due to its relatively low probability, it is only important at high electron densities. Next we have radiative recombination

$$e^- + X(Z,N-1) \longrightarrow X(Z,N) + h\nu \ . \tag{30}$$

This is just the reverse of photoionization, and it dominates the recombination cross section at relatively low electron energies; however, its importance decreases rapidly with energy. Finally, we have the indirect process of dielectronic recombination (DR)

$$e^- + X(Z,N-1) \longrightarrow X(Z,N)^{**} \longrightarrow X(Z,N) + h\nu \ . \tag{31}$$

This process involves resonant recombination to a doubly

excited state of the N-electron ion followed by radiative decay to a bound state. Of course, the doubly excited state can also autoionize and provide a resonance contribution to the elastic or excitation cross section of the (N-1)-electron ion. DR is the dominant recombination process at relatively high energies, and we shall now consider it in more detail.

In principle, radiative recombination and dielectronic recombination can interfere. A formalism to treat such interference has been developed;[19] however, model calculations[20] indicate that this will have a negligible effect on the total cross section. Furthermore, Bell and Seaton[21] have developed a coupled-channel formalism for DR, based on quantum-defect theory, which properly includes the interaction of the doubly excited states with the adjacent continuum, and with each other. However, the majority of calculations have been performed using an independent-processes approximation, and a comparison of results obtained with these two methods seems to indicate that the effects of overlapping, interfering resonances on the total-DR cross section are small.

In the isolated-resonance approximation, the DR cross section from an initial level i of the (N-1)-electron ion is given by

$$\sigma_{dr}(i) = \sum_j \sigma_r(i \rightarrow j) B_j^r \tag{32}$$

where again, $\sigma_r(i \rightarrow j)$ is the resonant-recombination cross section to a doubly excited level j of the N-electron ion. B_j^r is the branching ratio for radiative decay to a bound state of the N-electron ion. It is given by

$$B_j^r = \frac{\sum_n A_r(j \rightarrow n)}{\sum_k A_a(j \rightarrow k) + \sum_m A_r(j \rightarrow m)} , \tag{33}$$

where the sum over n is over all lower bound levels of the N-electron ion, while the sum over m is over all lower levels of the N-electron ion, bound and autoionizing.

As an example let us consider dielectronic recombination associated with the 2s $\longrightarrow$2p excitation in Li-like C^{3+}

$$e^- + C^{3+}(1s^2 2s) \longrightarrow C^{2+}(1s^2 2pn\ell) \longrightarrow C^{2+}(1s^2 2sn\ell) + h\nu$$
$$\hookrightarrow C^{2+}(1s^2 2pn'\ell') + h\nu'. \quad (34)$$

The radiative transitions involving the Rydberg electron ($n\ell \longrightarrow n'\ell'$) can dominate for low Rydberg states, but their importance falls off rapidly with the principal quantum number n. On the other hand, the radiatve rates for the transitions involving the core electron (2p$\longrightarrow$2s) are nearly independent of the Rydberg electron. An energy-level diagram for this system is shown in Fig. 7.

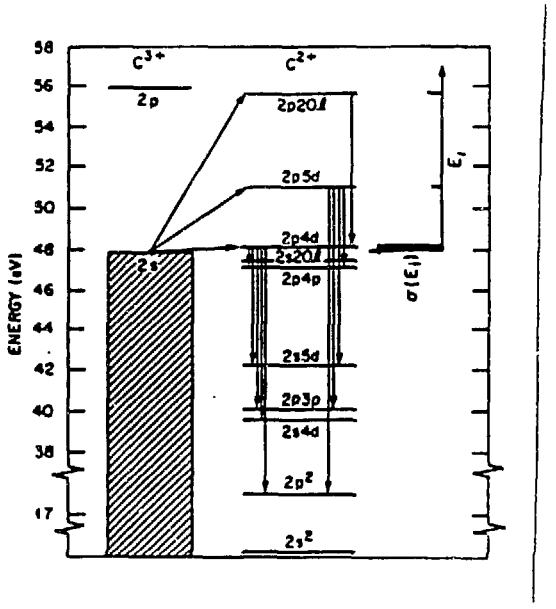

Fig. 7. An energy level diagram illustrating several DR transitions associated with the 2s$\longrightarrow$2p excitation in C^{3+}. A schematic diagram of the DR cross section resulting from transitions through the 2p4d, 2p5d, and 2p20ℓ configurations of C^{2+} is inset on the far right.

The low lying resonances such as 2p4d have relatively large cross sections because of the size of the radiative rates for transitions in which the Rydberg electron is the active electron; however, these resonances are rather widely spaced. On the other hand, the cross sections for the closely spaced high Rydberg states are smaller, but they continue to contribute to the cross section until we reach rather high values of the principal quantum number, n, where the resonant-recombination cross section (which falls of approximately as $1/n^3$) becomes so small that the states become essentially closed to recombination. Thus, the DR cross section associated with such $\Delta n = 0$ excitations are dominated by high Rydberg states.

External electric fields can have a pronounced effect on dielectronic recombination. First of all such fields can ionize electrons in high Rydberg states, and thereby decrease the DR cross section. Secondly, fields mix high Rydberg states with different values of the orbital angular momentum ℓ. The resonant recombination cross section is high for small values of ℓ and small for high values of ℓ, and in the absence of a field, the high angular momentum states are essentially closed to recombination. However external fields mix these states in such a way as to open up more channels for recombination and thereby enhance the cross section.

In DR experiments, the fields in the interaction region are relatively small, while the fields in the analyzing region are very large, typically of the order of 10 kV/cm. Thus the smaller fields in the interaction region enhance the DR cross section, and then after recombination has occurred, the fields in the interaction region strip off the high Rydberg states.

The amount of field ionization can be determined by employing hydrogenic field-ionization formulas such as the one developed by Damburg and Kolosov.[22] However, a much

simpler method to estimate the effects of field ionization is to assume that states rapidly ionize for all values of $n>n_m$, where the cutoff, n_m, is given by the semiclassical formula

$$n_m = \left[\frac{6.2 \times 10^5}{E} q^3 \right]^{1/4} , \tag{35}$$

where E is the electric field in V/cm and q is the charge of the ion before recombination. It has been found that the cutoff determined from this formula agrees closely with with the value of n for which the hydrogenic formulas predict a very rapid increase in the rate of field ionization.[23]

We determine the effects of field mixing in the interaction region by employing eigenvectors for the doubly excited states which are obtained by diagonalizing a Hamiltonian matrix that includes the stark matrix elements as well as the internal electrostatic and spin-orbit terms. Finally, the DR experiments do not measure the cross section, but rather the product of the electron velocity and the cross section convoluted with an electron velocity distribution function - a sort of rate coefficient which is a function of electron energy. Thus we combine our cross section with the experimental velocity distribution to make a theoretical prediction of the measurement.

The first DR measurements on a series of Li-like and Na-like ions were done by Dittner et al. at ORNL.[24,25] In this set of experiments, the field in the interaction region was expected to be about 30 V/cm. Although the agreement between experiment and our theoretical calculations[26] was quite good for the Na-like ions,[24] the measured rates were larger than the calculated rates for the Li-like ions (including the C^{3+} case considered above) even for the maximum field enhancement of the theoretical

cross sections.[25] Furthermore, the velocity distribution in these experiments was sufficiently wide that a comparison between experiment and theory was impossible for low Rydberg states, which are not affected by electric fields.

Andersen and Bolko have now completed measurements of DR for C^{3+} and O^{5+} using the Aarhus EN-tandem accelerator and a beamline equipped with an electron cooler.[27] The electric field in the interaction region is expected to be less than 5V/cm and the electron distribution is very narrow, so that individual low Rydberg states are resolved.

Their measurements for C^{3+} in comparison with our most recent calculations for various small fields in the interaction region[28] are shown in Fig. 8. As can be seen, the agreement between experiment and theory in the region of the high Rydberg states for energies between 7.0 and 8.0 eV is excellent for a field of about 3 V/cm. However, the

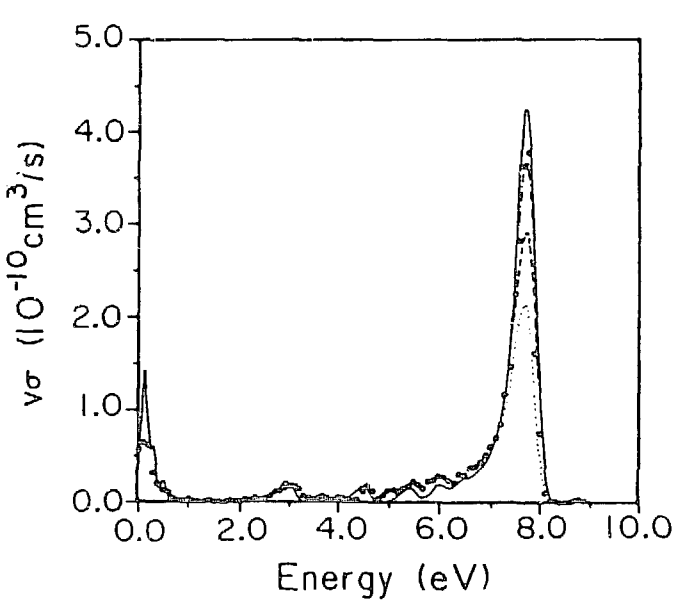

Fig. 8. Theoretical DR rate coefficients for C^{3+} (as measured in the Aarhus electron-ion merged-beam experiment) as a function of electron energy. ····· E = 0 V/cm; - - - E = 1 V/cm; -·-·-·- E = 3 V/cm; ———— E = 5 V/cm. The calculations include all resonances up to and including n_m = 35. The experimental points are from Ref. 27.

calculated rate for the peak between 0 and 0.6 eV, which is due to the 2p4d and 2p4f resonances, is nearly twice the measured rate. Since the cross section for resonant recombination varies as the inverse of the electron energy (see Eq. 15), and these resonances lie so close to zero, this discrepancy is most likely due to errors in the calculated positions of the doubly excited levels for these configurations. The agreement with experiment for O^{5+} is not quite as good, but still very reasonable.[27,28]

Additional experiments using electron coolers and ion storage rings are now being planned for more highly ionized species, and they will provide further tests of our understanding of electron-ion recombination.

5. CONCLUSIONS

Doubly excited autoionizing states play an extremely important role in electron-ion collisions. They are populated as intermediate states during electron-impact excitation, ionization and recombination. They are included in a natural way when one employs close-coupling wave functions, but in many cases, the independent-processes approximation provides a reliable means for determining total cross sections. However, as more sensitive electron-ion collision experiments are developed, more interference effects between channels will be detected, and theoretical methods which include the interaction between the doubly excited states and the adjacent continuum will be necessary.

6. ACKNOWLEDGMENTS

We wish to thank D. C. Gregory for providing us with his data on the ionization of Ti^{11+} prior to publication, A. Müller for providing us with his data on ionization of

Li^+ prior to publication, and L. Andersen and J. Bolko for furnishing us with their data on DR for C^{3+} and O^{5+} prior to publication. Conversations with M. H. Chen and K. J. Reed regarding the calculation of resonant recombination double autoionization in Fe^{15+} are also gratefully acknowledged. This work was supported by the Office of Fusion Energy, U. S. Department of Energy, under Contract No. DE-AC05-84OR21400 with Martin Marietta Energy Systems, Inc. and Contract No. DE-FG05-86ER53217 with Auburn University.

REFERENCES

1. Mitroy, J., Griffin, D. C., Norcross, D. W., and Pindzola, M. S., Phys. Rev. A38, 3339 (1988).
2. Pindzola, M. S. and Griffin, D. C., Phys. Rev. A39, 2385 (1989).
3. Cowan, R. D., J. Phys. B13, 1471 (1980).
4. Pindzola, M. S., Griffin, D. C., and Bottcher, C., Phys. Rev. A32, 822 (1985).
5. Peterkop, R. K., Zh. Eksp. Teor. Fiz. 41, 1938 (1961) [Sov. Phys. - JETP 14, 1377 (1962)].
6. Jakubowicz, H. and Moores, D. L., J. Phys. B14, 3733 (1981).
7. Moores, D. L. and Reed, K. J., Phys. Rev. A39, 1747 (1989).
8. Pindzola, M. S., Griffin, D. C., and Bottcher, C., submitted to Phys. Rev. A (1989).
9. Griffin, D. C., Pindzola, M. S., and Bottcher, C., Phys. Rev. A36, 3642 (1987).
10. Gregory, D. C., Wang, L. J., Rinn, K., and Meyer, F. W., Phys. Rev. A35, 3256 (1987).
11. Gregory, D. C., Wang, L. J., and S. Chantrenne, private communications.

12. LaGattuta, K. J. and Hahn, Y., Phys. Rev. A24, 2273 (1981).
13. Chen, M. H. and Reed, K. J., private communication.
14. Pindzola, M. S. and Griffin, D. C., Phys. Rev. A36, 2628 (1987).
15. Müller, A., Hoffmann, G., Tinschert, K., and Salzborn, E., Phys. Rev. Letts., 61, 1352 (1988).
16. Müller, A., Hofmann, G., Weissbecker, B., Stenke, M., Tinschert, K., Wagner, M., and Salzborn, E., private communication.
17. Fano, U., Phys. Rev. 124, 1866 (1961).
18. Cress, M. A., Seaton, M. J., and Wilson, P. M. H., Comput. Phys. Commun. 15, 23 (1978).
19. Alber, G., Cooper, J., and Rau, A. R. P., Phys. Rev. A30, 2845 (1984).
20. Griffin, D. C. and Pindzola, M. S., Phys. Rev. A35, 2821 (1987).
21. Bell, R. H. and Seaton, M. J., J. Phys. B18, 1589 (1985).
22. Damburg, R. J. and Kolosov, V. V., J. Phys. B12, 2637 (1979).
23. Bottcher, C., Griffin, D. C., and Pindzola, M. S., Phys. Rev. A34, 860 (1986).
24. Dittner, P. F., Datz, S., Miller, P. D., Pepmiller, P. L., and Fou, C. M., Phys. Rev. A33, 124 (1986).
25. Dittner, P. F., Datz, S., Miller, P. D., Pepmiller, P. L., and Fou, C. M., Phys. Rev. A35, 3668 (1987).
26. Griffin, D. C., Pindzola, M. S., and Bottcher, C., Phys. Rev. A33, 3124 (1986).
27. Andersen, L. H. and Bolko, J., submitted to Phys. Rev. A (1989).
28. Griffin, D. C., Pindzola, M. S., and Krylstedt, P., submitted to Phys. Rev. A (1989).